Progressive failure analysis of center-notched laminar composites in tension

Emilija Jočić[1], Miroslav Marjanović[1]
[1] Faculty of Civil Engineering, University of Belgrade, Bulevar kralja Aleksandra 73, 11000 Belgrade, Serbia
E-mail: edamjanovic@grf.bg.ac.rs, mmarjanovic@grf.bg.ac.rs

Abstract

This paper presents the application of the full-layerwise-theory (FLWT) in conjunction with the smeared crack-band (SCB) damage model for progressive failure analysis (PFA) of a center-notched tensile (CNT) laminar composite. The FLWT-SCB approach employs layered finite elements, enhancing computational efficiency while maintaining the accuracy of 3D finite elements. Both the initiation and modes of failure were determined using the Hashin failure criterion. The damaged lamina's response in both fiber and matrix directions was characterized by distinct bilinear strain-softening curves. To address mesh dependency, the fracture energy was scaled using a characteristic element length. A benchmark numerical study is presented to analyze the impact of specimen size on the tensile strength of center-notched laminar composites. To validate the model's effectiveness, results were compared against experimental and benchmark data from the literature, demonstrating excellent agreement. The model also revealed a weak dependency between the size of the structure and the mesh, and has a potential in analysis of bio-based composites such as CLT.

Keywords: progressive failure analysis, smeared crack band damage model, full layerwise theory

1 Introduction

Fiber-reinforced composites have been widely used in the construction of aerospace, marine, mechanical, and automotive structures for their remarkable strength, stiffness, low maintenance costs and corrosion resistance. These materials have a growing use in civil engineering, as well. However, optimal design with laminar composites is often driven by uncertainties in failure prediction, stemming from the complex nature of composite materials. Inherent variability in mechanical properties is common due to manufacturing processes, material inconsistencies, and environmental factors [1]. The complex kinematics of laminar composites can lead to various failure scenarios, including fiber breakage, pull-out, matrix yielding, cracking, and delamination [2]. In fiber-reinforced composites, damage progression typically initiates with matrix cracking transverse to the fibers, followed by fiber breakage and delamination between plies. The interaction of these failure mechanisms results in intricate crack pathways during damage propagation modeling. In real structural elements, joints, holes and notches are often present, which further complicates the prediction of damage progression due to the presence of stress concentration zones.

Progressive failure analysis (PFA) of laminar composites has been studied for a long time and used to predict damage progression and post-failure behaviour in composite materials. For the implementation of failure initiation and propagation algorithms within an existing numerical (i.e. finite element) model, damage models are required [3] such as: discrete damage models (DDM) and continuum damage models (CDM). Generally, discrete techniques lead to models that can accurately predict crack propagation with high fidelity, but at the cost of high computational effort. On the other hand, in CDM approaches, intralaminar cracks are

smeared out within the finite element domain and the fracture mechanism is then represented through material stiffness degradation, controlled by damage variables.

The earliest CDM approach is instantaneous softening method (ISM), where the material property associated with the failure model degrades instantly to zero (or some small value) of the undamaged material properties [4, 5]. A comparison of ISM-based models against the experimental results confirmed that the predicted failure occurs at a substantially lower load than the experimentally determined one, underestimating the laminate strength and neglecting the fact that the damage is indeed localized and a failed lamina still has a solid residual load-carrying capability.

Composite materials generally exhibit quasi-brittle post-failure behaviour resulting in a high fracture energy dissipated and therefore a more gradual propagation of fracture [6, 7]. An alternative approach to ISM is gradual softening method (GSM), where the material property associated with the failure mode is degraded gradually (i.e. linearly or exponentially) until it reaches zero [8-10]. GSM are very popular due to their simple implementation in commercial engineering software's based on the finite element method (FEM) and relatively low computational cost. However, the approaches outlined above suffer from a mesh dependency problem related to strain localisation during the PFA.

The mesh dependency issue can be overcome via the fracture-mechanics augmented smeared crack-band (SCB) model [11], by scaling the fracture energy using a characteristic element length, as described by the crack-band theory [12]. This approach was originally developed for the macroscopic sub-laminate level modeling of laminar composites [13]. However, the damage pattern and damage growth trajectory in orthotropic laminar composites cannot be realistically predicted, because the above damage model does not account for any preferred material orientation. Using the above model, the mesh orientation issue in SCB models was improved by devolving the sub-laminate strain softening response into equivalent stress-strain responses in the principal lamina directions [11, 14]. Such model leads to a good compromise between computational cost and solution accuracy, and they are thus used in most of the works dealing with composite failure modelling in conjunction with different plate theories [15]. However, the computational costs associated with PFA of laminar composites can be prohibitive, even considering the relative efficiency of SCB models, especially for larger structures. This is usually due to the requirement of refined, often 3D meshes, to obtain an accurate stress field.

This paper aims to increase the computational efficiency of the PFA of laminar composites and preserve the accuracy of the 3D finite element models, by using a layered FLWT-based finite element model [16] for structural analysis and SCB damage model [11] for material modelling. The use of FLWT is also justified due to the capability to account for continuous transverse (interlaminar) stresses between the adjacent layers in the laminate. The additional incorporation of transverse normal stress is crucial for modeling localized effects, such as holes, cut-outs, or the stress-deformation state around point supports where damage initiation is most likely to occur. The proposed FLWT-SCB prediction model was previously developed by authors [17] for the progressive failure modelling of open-hole laminar composites under tension, and applied here for PFA of a center-notched tensile (CNT) laminar composite. The developed FLWT-SCB prediction model was implemented into an original FLWTFEM framework [18], offering a user-friendly graphical environment for easy visualization of input and output data. A benchmark numerical study is presented to analyze the impact of specimen size on the tensile strength of center-notched laminar composites. To validate model's effectiveness, results were compared against experimental and benchmark data from the literature.

2 Layerwise theory for 3D structural analysis of laminar composites

In the paper, a laminated composite plate made of n perfectly bonded orthotropic layers is considered (Figure 1, left). The total plate thickness is denoted as h, while the thickness of the k^{th} lamina is denoted as h_k. The plate is supported along the portion Γ_u of the boundary Γ and loaded with loadings $q_t(x,y)$ and $q_b(x,y)$ acting to either top or the bottom surface of the plate (S_t or S_b). Piece-wise linear variation of all three displacement components through the thickness is imposed, leading to the layer-wise 3D stress field. The displacement field (u, v, w) of an arbitrary point (x,y,z) of the laminate is given as:

$$u(x,y,z) = \sum_{I=1}^{N} U^I(x,y)\Phi^I(z)\,,\ v(x,y,z) = \sum_{I=1}^{N} V^I(x,y)\Phi^I(z)\,,\ w(x,y,z) = \sum_{I=1}^{N} W^I(x,y)\Phi^I(z) \quad (1)$$

In Eq. (1), N is the number of numerical layers, $U^I(x,y)$, $V^I(x,y)$ and $W^I(x,y)$ are the displacement components in the I^{th} numerical layer of the plate in directions x, y and z, respectively, $\Phi^I(z)$ are selected to be linear layerwise continuous functions of the z-coordinate, defined over the considered layer I.

Based on the assumed displacement field, linear strain field can be easily derived and may be found in [16]. To reduce the 3D model to a plate model, the *z*-coordinate is eliminated by the explicit integration of stresses multiplied with the corresponding functions $\Phi^I(z)$, introducing the constitutive relations of the laminate which can be found in [16].

The finite element discretization is derived by introducing an assumed interpolation of the displacement field into the weak form of the FLWT. All displacement components are interpolated using the same 2-D Lagrange interpolation polynomials. Element stiffness matrix is obtained in a common way, using 2D Gauss-Legendre quadrature for quadrilateral domains. In the paper, quadratic serendipity (Q8) layered quadrilateral elements have been considered (Figure 1, right). To avoid shear locking, reduced integration is used (2×2 points for Q8). After the derivation of the characteristic element matrices, the assembly procedure is performed in a usual manner.

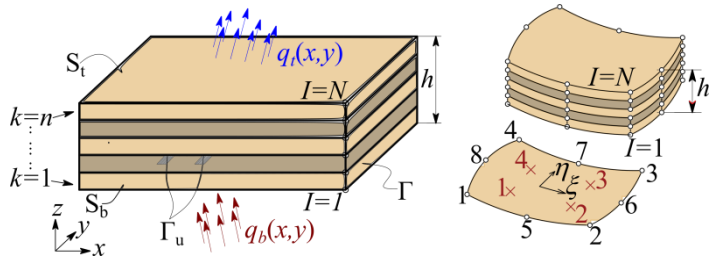

Figure 1: left: Laminated composite plate; right: Quadratic serendipity Q8 layered element

Once the nodal displacements are obtained the stresses are evaluated from the well-known lamina 3D constitutive equation in the Gauss points at the top (t) and bottom (b) interfaces of the considered lamina and they are given in [16]. The stresses are calculated both in the laminate (*xyz*) and the local lamina (*123*) coordinate systems. This is crucial in the progressive failure analysis (PFA), since the failure criteria require the stresses in the lamina coordinate system. Since the interlaminar stresses calculated from the constitutive equations are discontinuous at layer interfaces, they are re-computed by assuming quadratic distribution through each layer, using the procedure given in detail in [19].

3 Smeared crack band damage model

The nonlinear material behaviour is described via the fracture-mechanics augmented SCB damage model, where both the failure initiation and the failure modes are determined using the Hashin failure criterion [20]. The SCB damage model has been previously described in [17] and is briefly recapitulated here for completeness.

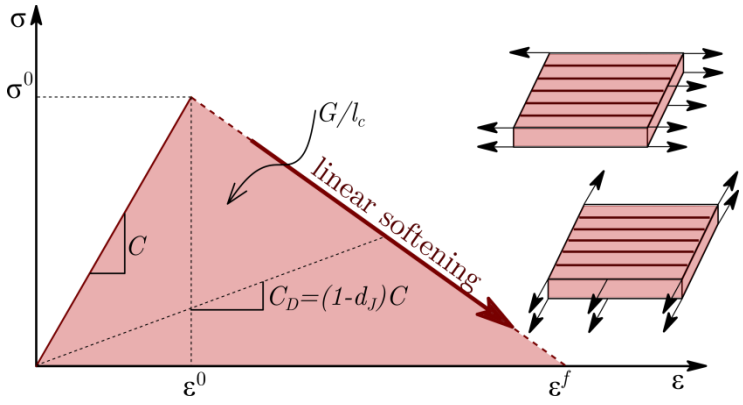

Figure 2: Stress-strain relationship with linear softening

In smeared formulations, the fracture energy is distributed (smeared) over the full volume of the element. The response of damaged lamina, in both fiber and matrix direction, was described by distinct bilinear strain-softening curves (see Figure 2), where the peak stress coincides with the fibre and matrix strength, respectively. This damage law is determined based on the assumption that the total energy needed to fail an element (released strain energy) is equal to the energy needed to create a crack that passes through it. The

released strain energy of a failed element is determined as a product of the area under the stress-strain curve, defined in Figure 2, and characteristic element length l_c. In the present work, l_c is defined as the square root of a layered finite element area. This energy is set to be equal to the dissipated fracture energy of the composite material (fracture toughness):

$$\varepsilon^f = 2G/\sigma_0 l_c \tag{2}$$

In Eq. (2), ε^f is maximum strain, while σ_0 is the material strength. The fracture toughness G is a material property that must be specified for each failure mode. By including the characteristic element length into the material damage law, the constant dissipated fracture energy is achieved, regardless of the element dimensions.

The material stiffness degradation is controlled by damage variables, each ranging between zero (undamaged status) and one (complete damaged status) for the corresponding damage mode. The evolution of each damage variable is governed by equivalent strain $\varepsilon_{J,eq}$. In this way, each damage mode is represented as a 1D stress-strain problem (Figure 2) instead of the actual 3D stress-strain relation. The equivalent strain and corresponding equivalent stress for each failure mode were defined in detail in [17]. Using the equivalent strain and stress, a damage variable for each failure mode J (J = fiber tension, fiber compression, matrix tension, matrix compression) can be calculated using the following relation:

$$d_J = \frac{\varepsilon^f_{J,eq}\left(\varepsilon_{J,eq}-\varepsilon^0_{J,eq}\right)}{\varepsilon_{J,eq}\left(\varepsilon^f_{J,eq}-\varepsilon^0_{J,eq}\right)} \tag{3}$$

In Eq. (3), $\varepsilon^0_{J,eq}$ is the equivalent strain at the initial failure state ($d_J = 0$) and $\varepsilon^f_{J,eq}$ is the equivalent strain at the final failure state ($d_J = 1$). Since damage evolution is an irreversible process, damage variable is equal to the maximum of its current value and the value obtained from Eq. (3). The equivalent strain at the final failure state $\varepsilon^f_{J,eq}$ is computed from Eq. (2).

4 Model validation, results and discussion

In the validation example, the FLWT-SCB prediction model is applied to predict damage progression and the strength of a center-notched tensile (CNT) laminar composite. The configuration of the laminate is illustrated in Figure 3, left, and consists of 32 layers of thickness h_k = 0.125 mm, assembled in $[45^o/90^o/-45^o/0^o]_{4s}$ stacking sequence. One end of the coupon is constrained while a displacement u is imposed on the opposite end. The material used in this example is IM7/8552 carbon fibre reinforced polymer (CFRP) with material properties provided in Table 1.

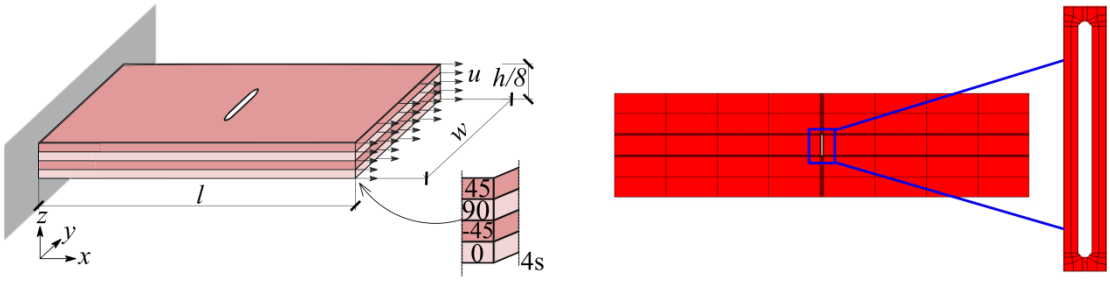

Figure 3: left: Geometry and boundary conditions of the CNT laminar composite; right: Generated mesh with 138 Q8 layered quadrilateral elements

Table 1: Material properties for IM7/8552 carbon fibre reinforced polymer

E_1 (GPa)	$E_2 = E_3$ (GPa)	$G_{12} = G_{13}$ (GPa)	G_{23} (GPa)	$\nu_{12} = \nu_{13}$	ν_{23}	X_t (MPa)	X_c(MPa)
147.7	8.52	4.59	3.91	0.3	0.38	2737	1600
$Y_t = Z_t$ (MPa)	$Y_c = Z_c$ (MPa)	$S = T$ (MPa)	R (MPa)	G_{ft} (KJ/m^2)	G_{fc} (KJ/m^2)	G_{mt} (KJ/m^2)	G_{mc} (KJ/m^2)
51.32	201.08	81	65	180	100	0.3	1.71

To showcase the capability of the FLWT-SCB framework in forecasting size effects in laminar composites, multiple sizes of the specimen have been numerically analysed. Table 2 comprises a list of employed scales and their dimensions. The present example has been verified using the research of Nagaraj et al. [21], which use SCB for damage modelling and higher-order theories based on Carrera Unified Formulation (CUF) for structural modelling [22]. Additionally, the maximum strengths estimated in the current example have been also experimentally validated [23].

Table 2: List of employed scales and their dimensions

Scale	Notch length c [mm]	Specimen Width w [mm]	Specimen Length l [mm]
1	3.2	15.9	63.5
2	6.4	31.8	127
4	12.7	63.5	254
8	25.4	127	508
16	50.8	254	508

The numerical analysis was performed using 138 Q8 layered quadrilateral elements, with only a small area surrounding the notch being refined with smaller elements (see Figure 3, right). The fracture process zone has a mesh size of roughly 0.5 x 0.5 mm for the scale-8 mesh. Due to symmetry in stacking sequence, only a half of the laminate was modelled to reduce the number of finite elements. At the clamped edge, all DOFs were restricted, while in the symmetry plane, displacements in the thickness direction were set to zero. The laminae were treated as a single numerical layer, with a linear distribution of displacements across the thickness of the lamina. The element distribution remained constant for all CNT specimens, with the element edge size scaling according to the specimen's dimensions.

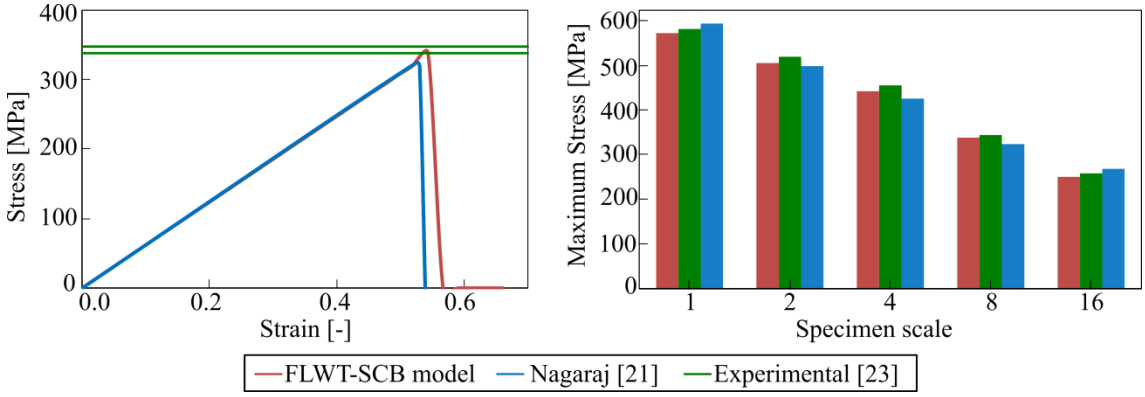

Figure 4: left: Tensile stress – strain curves of a center-notched specimen (Scale-8); right: Comparison of maximum stress values for all CNT specimens

Table 3: Comparison of maximum stress values for all CNT specimens using FLWT-SCB framework, Nagaraj's model [21], and experimental data [23]

Scale	FLWT-SCB	Nagaraj [21]	Experimental [23]	Δ^a[%]	Δ^b[%]
1	572.3	593.2	581.4	1.6	2.0
2	505.3	498.3	519.1	2.6	4.1
4	442.3	425.6	455.3	2.9	6.5
8	338.3	323.9	344.1	1.7	5.9
16	250.3	268.4	258.1	3.0	4.0

[a] Percentage relative difference of proposed model compared to experimental data
[b] Percentage relative difference of reference numerical model [23] compared to experimental data

Figure 4, left displays a typical stress-strain curve for a scale-8 CNT sample, as predicted by both the FLWT-SCB framework and Nagaraj's model [21]. The minimum and maximum strength values obtained from experiments [23] are indicated by green horizontal lines. Figure 4, left shows that the specimen exhibits a brittle behaviour, characterized by a linear elastic rise in stress up to the maximum value, followed by an abrupt decrease in stiffness leading to failure. The results obtained from the current approach are consistent with both numerical and experimental reference results. According to Nagaraj's model (blue line), the CNT sample's tensile strength is expected to be 323.9 MPa, which is approximately 5.9% lower than the experimental results. In contrast, when simulated using the FLWT-SCB framework (red line), the sample's

tensile strength is 338.3 MPa, which is in better agreement with experimental data (with an average relative difference of 1.7%). The stress-strain curves for the remaining CNT scaled specimens are not included here because they are similar to the data presented in the Figure 4, left. Instead, the maximum stress obtained by FLWT-SCB along with the experimental and reference numerical results, for all scales, have been presented in Table 3 and plotted in Figure 4, right. Based on Figure 4 and Table 3, right, it becomes evident that FLWT SCB consistently forecasts tensile strengths that are more similar to the experimental data compared to Nagaraj's [21] results.

5 Conclusions and future work

In the paper, a novel FLWT-SCB prediction model was successfully applied in the progressive failure analysis (PFA) of a center-notched tensile (CNT) laminar composite. The model employs layered finite elements, enhancing computational efficiency while maintaining the accuracy of 3D finite elements. The developed model was implemented into an original FLWTFEM framework, offering a user-friendly graphical environment for easy visualization of input and output data. In SCB approaches, the material stiffness matrix degradation was controlled by damage variables, which evolution are governed by an equivalent strains appropriately defined for each failure mode. The response of damaged lamina, in both fiber and matrix direction, was described by distinct bilinear strain-softening curves, where the peak stress coincides with the fibre and matrix strength, respectively. The mesh dependency problem was reduced by scaling the fracture energy using a characteristic element length, as described by the crack-band theory. Both the initiation and modes of failure were determined using the Hashin failure criterion. The use of layered quadrilateral elements in the damage modelling of laminar composites is relatively unexplored in the literature, where the standard approach is to use linear solid elements.

A benchmark numerical study is presented to analyze the impact of specimen size on the tensile strength of center-notched laminar composites. The numerical analysis was performed using 138 Q8 layered quadrilateral elements, with only a small area surrounding the notch being refined with smaller elements which significantly reduced the number of DOFs of the considered problem. To validate the model's effectiveness, results were compared against experimental and benchmark data from the literature.

The FLWT-SCB model demonstrated a brittle behaviour of center-notched tensile specimen, with a linear elastic increase of the load until reaching the peak value, followed by an abrupt loss of stiffness leading to failure. The results obtained from the current approach are consistent with both numerical and experimental reference results. Also, the FLWT-SCB prediction model showed consistent prediction of tensile strengths in center-notched laminar composites, which closely align with experimental data, in contrast to the reference numerical results. The mesh discretization remained constant for all specimens without compromising accuracy or significantly affecting computational time.

The advantages of layered FLWT-based finite element model were demonstrated, in particular the savings in computational costs and the capability to provide the accurate 3D stress field, which is curious for accurate prediction of damage initiation and evolution in problems with highly localized stress peaks. Moreover, the use of layered quadrilateral elements leads to relaxation of element aspect-ratio and size constraints, from which 3D models suffer. These aspects could have significant advantages in improving the computational efficiency during the progressive failure analysis of large-scale composite structures.

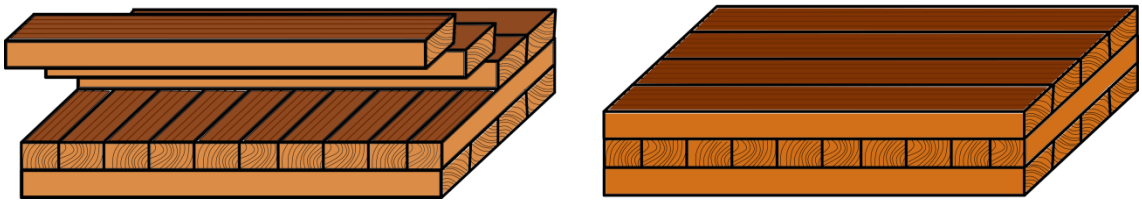

Figure 5: Cross laminated timber (CLT) panel

Future efforts will focus on expanding the capabilities of the FLWT-SCB framework to address the PFA of cross-laminated timber (CLT) panels. This extension involves adapting strain-softening curves to account for different post-failure behaviour of timber in tension and compression. By doing so, the computational framework's applicability will be expanded to include the field of computational mechanics for bio-based

composites. This development is in line with the growing prevalence of bio-based composites in building construction, reflecting the increasing awareness of environmental protection in the 21st century.

Acknowledgments

This research was supported by the Science Fund of the Republic of Serbia, GRANT No. 7677448: Towards Sustainable Buildings: Novel Strategies for the Design of Vibration Resistant Cross-Laminated Timber Floors - Substrate4CLT.

References

[1] J. P. Torres, L.-J. Vandi, M. Veidt, M.T. Heitzmann. The mechanical properties of natural fibre composite laminates: A statistical study. *Composites Part A: Applied Science and Manufacturing*, 98: 99–104, 2017. doi: 10.1016/j.compositesa.2017.03.010.

[2] O.O. Ochoa, J. N. Reddy. *Finite Element Analysis of Composite Laminates*. 1992.

[3] A. C. Orifici, I. Herszberg, R. S. Thomson. Review of methodologies for composite material modelling incorporating failure. *Composite Structures*, 86(1-3): 194–210, 2008. doi: 10.1016/j.compstruct.2008.03.007.

[4] S. C. Tan. A progressive failure model for composite laminates containing openings. *Journal of Composite Materials*, 25(5): 556–577, 1991. doi: 10.1177/002199839102500505.

[5] P. P. Camanho, F. L. Matthews. A progressive damage model for mechanically fastened joints in composite laminates. *Journal of Composite Materials*, 33(24): 2248–2280, 1999. doi: 10.1177/002199839903302402.

[6] M. J. Laffan, S. T. Pinho, P. Robinson, L. Iannucci. Measurement of the in situ ply fracture toughness associated with mode I fibre tensile failure in FRP. Part I: Data reduction. *Composites Science and Technology*, 70: 606–613, 2010. doi: 10.1016/j.compscitech.2009.12.016.

[7] M. J. Laffan, S. T. Pinho, P. Robinson, L. Iannucci. Measurement of the in situ ply fracture toughness associated with mode I fibre tensile failure in FRP. Part II: Size and lay-up effects. *Composites Science and Technology* 70: 614–621, 2010. doi: 10.1016/j.compscitech.2009.12.011.

[8] F. K. Chang, K. Y. Chang. A progressive damage model for laminated composites containing stress concentrations. *Journal of Composite Materials*, 21: 834–855, 1987. doi: 10.1177/002199838702100904.

[9] Y. W. Kim, C. S. Hong. Progressive Failure Model for the Analysis of Laminated Composites Based on Finite Element Approach. *Journal of Reinforced Plastics and Composites*, 11(10): 1078–1092, 1992. doi: 10.1177/073168449201101001

[10] Y. S. N. Reddy, C. M. D. Moorthy, J. N. Reddy. Non-linear progressive failure analysis of laminated composite plates. *International Journal of Non-Linear Mechanics*, 30(5): 629–649, 1995. doi: 10.1016/0020-7462(94)00041-8.

[11] A. Forghani, A. Poursartip, R. Vaziri R. An orthotropic non-local approach to modeling intra-laminar damage progression in laminated composites. *International Journal of Solids and Structures*, 180: 160–175, 2019. doi: 10.1016/j.ijsolstr.2019.07.015.

[12] Z. P. Bazant. Instability, ductility, and size effect in strain-softening concrete. *Journal of Engineering Mechanics – Asce*, 102(2): 331–344, 1976. doi: 10.1061/JMCEA3.0002111.

[13] K. V. Williams, R. Vaziri, A. Poursartip. A physically based continuum damage mechanics model for thin laminated composite structures. *International Journal of Solids and Structures*, 40(9): 2267–2300, 2003. doi: 10.1016/j.ijsolstr.2019.07.015.

[14] J. Reiner, T. Feser, D. Schueler, M. Waimer, R. Vaziri. Comparison of two progressive damage models for studying the notched behavior of composite laminates under tension. *Composite Structures*, 207: 385–396, 2019. doi: 10.1016/j.compstruct.2018.09.033.

[15] M. H. Nagaraj, J. Reiner, R. Vaziri, E. Carrera, M. Petrolo. Compressive damage modeling of fiber-reinforced composite laminates using 2D higher-order layer-wise models. *Composites Part B: Engineering*, 215: 108753, 2021. doi: 10.1016/j.compositesb.2021.108753.

[16] J. N. Reddy. *Mechanics of laminated composite plates and shells: theory and analysis*. Boca Raton, Florida: CRC Press, 2004.

[17] E. Jočić, M. Marjanović. Progressive failure analysis of open-hole composite laminates using FLWT-SCB prediction model. *International Journal of Mechanical Sciences*, 227: 107407, 2022. doi: 10.1016/j.ijmecsci.2022.107407.

[18] M. Marjanovic, G. Meschke, E. Damnjanovic. Object-oriented framework for 3D bending and free vibration analysis of multilayer plates: Application to cross-laminated timber and soft-core sandwich panels. *Composite Structures*, 255: 112–159, 2021. doi: 10.1016/j.compstruct.2020.112859.

[19] M. Marjanovic, N. Markovic, E. Damnjanovic, R. Cvetkovic. Three-dimensional stress analysis and design of cross-laminated timber panels using full-layerwise-theory-based finite element method. *Thin-Walled Structures*, 157: 107–156, 2020. doi: 10.1016/j.tws.2020.107156.

[20] Z. Hashin. Failure criteria for unidirectional fibre composites. *ASME Journal of Applied Mechanics*, 47: 329–334, 1980. doi: 10.1115/1.3153664.

[21] M. H. Nagaraj M, J. Reiner, R. Vaziri, E. Carrera, M. Petrolo. Progressive damage analysis of composite structures using higher-order layer-wise elements. *Composites Part B: Engineering*, 190: 107921, 2020. doi: 10.1016/j.compositesb.2020.107921.

[22] E. Carrera, M. Cinefra, M. Petrolo, E. Zappino. *Finite element analysis of structures through unified formulation*. Hoboken, New Jersey, United States: John Wiley & Sons, 2014. doi: 10.1002/9781118536643.

[23] X. Xu, M. R. Wisnom, X. Li, S. R. Hallett. A numerical investigation into size effects in centre-notched quasi-isotropic carbon/epoxy laminates. *Composites Science and Technology*, 111:32–39, 2015. doi: 10.1016/j.compscitech.2015.03.001.